Phase behaviour of blends of homopolymers with α-methylstyrene/acrylonitrile copolymers

P. P. Gan and D. R. Paul*
Department of Chemical Engineering and Center for Polymer Research, University of Texas at Austin, Austin, TX 78712, USA

and A. R. Padwa
Monsanto Chemical Co., Springfield, MA 01151, USA
(Received 22 June 1993; revised 16 September 1993)

This paper examines in detail the phase behaviour of blends of α-methylstyrene/acrylonitrile copolymers (α-MSAN) with poly(methyl methacrylate) (PMMA), tetramethylbisphenol A polycarbonate (TMPC), poly(vinyl chloride) (PVC), poly(2,6-dimethyl-1,4-phenylene oxide) (PPO), poly(ε-caprolactone) (PCL) and bisphenol A polycarbonate (PC), and compares these with the corresponding behaviour of blends based on styrene/acrylonitrile copolymers (SAN). Replacement of styrene with α-methylstyrene widens the miscibility window with PMMA and PVC but narrows the miscibility window with TMPC. In addition, the phase separation temperatures for α-MSAN blends with PVC are higher while those with PMMA and TMPC are lower compared to similar SAN-based blends. PPO, PCL and PC were found to be not miscible with any of the α-MSAN copolymers. Interaction parameters for these systems were evaluated where possible from their lower critical solution temperature type phase boundary using the lattice fluid theory of Sanchez and Lacombe. The interactions between various monomer unit pairs were deduced using a binary interaction model for copolymers. The interaction parameters obtained are translatable from one system to another. The results are discussed in terms of interactions between monomer unit pairs and equation-of-state or compressibility effects.

(Keywords: homopolymer–copolymer blends; acrylonitrile copolymers; phase behaviour)

INTRODUCTION

There has been considerable interest recently in blends involving copolymers and especially in the problem of mapping the composition boundaries that divide miscible from immiscible behaviour[1–26]. Frequently, these boundaries are used to estimate information about the interaction energies between monomer unit pairs by fitting them to the form predicted by a binary interaction model combined with the Flory–Huggins theory[1–3,6–9,18,20–25,27–31]. Owing to the mathematical nature of this problem, it is well known[1–4,6–9,12,18,26,28–30,32] that this approach alone cannot lead to the independent determination of the interaction energy parameters between all of the monomer unit pairs involved because the fitting procedure involves more parameters than experimental information. Generally, at least one parameter is taken from another source, which means that each parameter subsequently evaluated includes all of the uncertainties of this value. A case in point is the frequent use of the polystyrene–poly(methyl methacrylate) interaction parameter reported by Fukuda *et al.*[33–35] in the analysis of copolymers containing these monomers[1–4,18,36]. Often these experiments produce information in the form of phase diagrams stemming from lower critical solution temperature (*LCST*) behaviour that is not fully used in the analysis since the Flory–Huggins theory does not predict *LCST* behaviour without *ad hoc* empirical modifications[2–4,36]. As demonstrated recently[13–15], combining the binary interaction model with an appropriate equation-of-state theory that does predict *LCST* behaviour leads to a theoretical framework that allows use of this phase diagram information in addition to the composition boundaries. In favourable cases, this approach permits independent evaluation of all interaction energies between monomer pairs.

The phase behaviour of blends of homopolymers with styrene/acrylonitrile copolymers (SAN) has been extensively reported. Some preliminary studies have shown that substituting α-methylstyrene for the styrene in SAN copolymers leads to rather different phase behaviour. To date, blends of the α-methylstyrene/acrylonitrile copolymer (α-MSAN) at the azeotrope composition of 30 wt% AN have been explored extensively[21–25]. However, studies using other compositions of α-MSAN copolymers are more limited. This is due in part to the difficulties involved in synthesizing certain off-azeotrope α-MSAN copolymers with high molecular weight. Since the ceiling temperature for α-methylstyrene is 61°C[37], polymerization of compositions rich in this monomer is limited to lower temperatures to achieve high molecular weights. When the polymerization temperatures are so

* To whom correspondence should be addressed

0032-3861/94/07/1487–16

low, free-radical polymerization rates are exceedingly slow. Therefore, high molecular weights at low AN contents are difficult to obtain owing to the low ceiling temperature. Recently, studies of blends of α-MSAN copolymers with poly(alkyl acrylate)s, poly(alkyl methacrylate)s, poly(di-alkyl itaconates)s, alkyl methacrylate copolymers and styrene copolymers have been reported[8]. Another study has reported on the miscibility window for blends with PMMA[38]. However, the molecular weights of the α-MSAN copolymers used were rather low, which can significantly raise the phase separation temperature. This will affect the region of miscibility observed and the calculation of binary interaction energies if proper allowances are not made.

In this paper, the phase behaviour of blends of poly(methyl methacrylate) (PMMA), poly(vinyl chloride) (PVC), tetramethylbisphenol A polycarbonate (TMPC), poly(2,6-dimethyl-1,4-phenylene oxide) (PPO), poly(ε-caprolactone) (PCL) and low-molecular-weight polycarbonate (PC) with SAN copolymers are compared to those with α-MSAN copolymers prepared by procedures that yielded materials of relatively high molecular weight and uniform composition. A main goal is to obtain information about interaction energies between polymer segment pairs and to compare them with values obtained from various other sources where possible.

BACKGROUND AND THEORY

The Flory–Huggins theory[39], originally developed for polymer solutions, is the simplest model for describing polymer–polymer mixtures. The theory assumes that the only contribution to the entropy of mixing is combinatorial in origin and that the heat of mixing is represented by a van Laar type expression. The free energy of mixing of polymers A and B is given by:

$$\Delta G_{mix} = RT\left(\frac{\phi_A \ln \phi_A}{\tilde{V}_A} + \frac{\phi_B \ln \phi_B}{\tilde{V}_B}\right) + B\phi_A\phi_B \qquad (1)$$

where ϕ_i is the volume fraction and $\tilde{V}_i$ is the molar volume of component i. Differentiation of equation (1) gives the spinodal condition:

$$\frac{d^2\Delta g}{d\phi_1^2} = RT\left(\frac{1}{\phi_A\tilde{V}_A} + \frac{1}{\phi_B\tilde{V}_B}\right) - 2B_{sc} = 0 \qquad (2)$$

where B_{sc} is the interaction parameter at the spinodal condition. The term B_{sc} is equivalent to B in equation (1) if the latter is independent of composition[40]. However, the form of equation (2) is often used when B does depend on concentration, which amounts to the introduction of a new interaction energy, i.e.

$$B_{sc} = -\frac{1}{2}\frac{d^2\Delta g_{nc}}{d\phi_1^2} \qquad (3)$$

where Δg_{nc} is the non-combinatorial free energy. After this, we will primarily use this latter definition, but for simplicity the subscript 'sc' will be omitted except when needed for clarification or emphasis.

According to the binary interaction model[10,41,42], the net interaction energy B for mixing a random copolymer composed of units 1 and 2 and a homopolymer composed of units 3 is as follows:

$$B = B_{13}\phi'_1 + B_{23}\phi'_2 - B_{12}\phi'_1\phi'_2 \qquad (4)$$

where the B_{ij} describe the interaction between monomer units i and j. The volume fractions ϕ'_i are the close-packed volume fraction in the copolymer. A stability analysis for the case when the interaction energy is composition-independent shows that the blend is miscible provided that B is less than a critical value defined as follows:

$$B_{crit} = \tfrac{1}{2}RT(\tilde{V}_A^{-1/2} + \tilde{V}_B^{-1/2})^2 \qquad (5)$$

where $\tilde{V}_A$ and $\tilde{V}_B$ are the molar volumes of the copolymer and homopolymer, respectively.

Equation-of-state theories, e.g. the lattice-fluid theory of Sanchez and Lacombe[43–45], are more useful for present purposes than the Flory–Huggins theory since they predict *LCST* behaviour, which often arises from the compressible nature of the mixture. Using such a theory, information about phase separation temperatures can be used to aid the determination of interaction energies. The lattice-fluid equation of state has the following simple closed form:

$$\tilde{\rho}^2 + \tilde{P} + \tilde{T}[\ln(1-\tilde{\rho}) + (1-1/r)\tilde{\rho}] = 0 \qquad (6)$$

where the reduced properties are defined as $\tilde{P} = P/P^*$, $\tilde{T} = T/T^*$, $\tilde{\rho} = v^*/v$ and r is a chain length given by:

$$r = MP^*/kT^*\rho^* = M/\rho^*v^* \qquad (7)$$

For any polymer, the characteristic temperature T^*, pressure P^* and density ρ^* or hard-core segment volume v^* can be obtained by fitting *PVT* data to equation (6). Since the form of equation (6) does not precisely fit experimental *PVT* data over a wide range of pressure and temperature, it is common practice to use only relatively low-pressure data over limited temperature ranges. Thus, the values of the characteristic parameters depend on the temperature range employed (see *Table 2*). The following relations are used for mixtures and copolymers:

$$\begin{aligned}
P^* &= \phi_1 P_1^* + \phi_2 P_2^* - \phi_1\phi_2\Delta P^* \\
\frac{1}{v^*} &= \frac{\phi_1}{v_1^*} + \frac{\phi_2}{v_2^*} \\
\phi_1 &= \frac{m_1/\rho_1^*}{m_1/\rho_1^* + m_2/\rho_2^*} \\
v &= v_1^*/v_2^* \\
\frac{1}{\rho^*} &= \frac{m_1}{\rho_1^*} + \frac{m_2}{\rho_2^*} \\
\frac{T^*}{T} &= \frac{1}{\tilde{T}} = \frac{\phi_1/\tilde{T}_1 + v\phi_2/\tilde{T}_2}{\phi_1 + v\phi_2} - \frac{\phi_1\phi_2\Delta P^* v^*}{kT} \\
r_i^o v_i^* &= r_i v^*
\end{aligned} \qquad (8)$$

In analogy with equation (4), the net bare interaction energy for a blend of a copolymer and homopolymer, ΔP^*, is given by [28]:

$$\Delta P^* = \phi'_1\Delta P_{13}^* + \phi'_2\Delta P_{23}^* - \phi'_1\phi'_2\Delta P_{12}^* \qquad (9)$$

where ΔP_{ij}^* are the binary pair interaction energies, and ϕ'_1 and ϕ'_2 are the close-packed volume fraction of units 1 and 2 in the copolymer. The spinodal condition for a binary mixture is given by:

$$\frac{d^2G}{d\phi_1^2} = \frac{1}{2}\left(\frac{1}{r_1\phi_1} + \frac{1}{r_2\phi_2}\right) - \tilde{\rho}\left(\frac{\Delta P^* v^*}{kT} + \frac{1}{2}\psi^2\tilde{T}P^*\beta\right) = 0 \qquad (10)$$

where ψ is a dimensionless function described elsewhere[46]

and β is the isothermal compressibility factor. For high-molecular-weight polymers, the combinatorial entropy is negligible and, thus, the first term in equation (10) can be neglected. Portions of the second term are negligible; and after some rearrangement, the spinodal condition can be reduced to:

$$\frac{d^2G}{d\phi_1^2} = -\frac{\tilde{\rho}\Delta P^* v^*}{kT} - \frac{\tilde{\rho}}{2}\left(\frac{v(T_1^* - T_2^*)}{T(\phi_1 + v\phi_2)^2}\right)^2 \tilde{T}P^*\beta = 0 \quad (11)$$

Therefore, to a good approximation, the phase behaviour of polymer blends is governed by the above two terms in the spinodal equation.

MATERIALS AND PROCEDURES

The copolymerization of α-methylstyrene with acrylonitrile was carried out in bulk at 40°C using mixtures of t-butylperoxy-2-ethylhexanoate and t-butylperoxyneodecanoate (Lucidol Div., Atochem, Buffalo, NY) commensurate to the timescale of polymerization. For typical long-timescale polymerizations, i.e. polymers with less than 25 wt% AN, 0.05 wt% t-butylperoxy-2-ethylhexanoate and 0.008 wt% t-butylperoxyneodecanoate were used. For copolymers containing greater than 25 wt% AN, 0.1 wt% t-butylperoxyneodecanoate was used. The monomers were commercial polymerization grade. The inhibitors were removed with activated alumina (Scientific Polymer Products, Ontario, NY). The polymerization was carried out in 1 litre capped bottles, in which the monomers were nitrogen purged by bubbling at room temperature for about 5 min. After the required time to achieve approximately 1–2% conversion, the solution was concentrated on a rotary evaporator at 65°C using increasing vacuum levels to control the rate of evaporation. When most of the monomers were removed, the resulting viscous solution was diluted to an estimated 5 wt% concentration with 2-butanone (except that acetone was used for polymers with greater than 40 wt% AN) and reprecipitated by dropwise addition into five volumes of methanol in a high-speed blender. The vacuum-filtered moist polymer was redissolved to about 5 wt% concentration and precipitated again. The resulting polymer was dried overnight at 80°C in a vacuum oven with a nitrogen bleed.

Acrylonitrile content was estimated by automated Carlo-Erba CHN elemental analysis. Molecular weights, for copolymers containing less than 45 wt% AN, were estimated by g.p.c. in tetrahydrofuran using four columns containing a mixed pore-size bed of 5 μm beads (Polymer Laboratories, Amherst, MA). The flow rate was 1 ml min^{-1} at 35°C with a refractive index detector. Molecular weights are reported in polystyrene equivalents. For copolymers containing more than 45 wt% AN, the molecular weights were determined in hexafluoroisopropanol using both refractive index and laser light scattering detectors to determine absolute molecular-weight distributions. *Table 1* shows the molecular-weight information for α-MSAN copolymers and homopolymers used in this study.

All blends of α-MSAN copolymers were prepared by solution casting from tetrahydrofuran (THF) onto a heated glass plate at 60°C, unless mentioned otherwise. The cast films were dried at 60°C for about 10 min, before further drying in the vacuum oven at a temperature of 20 to 30°C higher than the glass transition of the blend (T_g). If this produced phase-separated blends, other solvents or other methods of preparation were attempted.

Glass transition temperatures were measured using a Perkin–Elmer DSC-7 at a scanning rate of 20°C min^{-1}. The onset of the change in heat capacity was defined as the T_g. The temperatures at which phase separation occurs on heating, i.e. *LCST* behaviour, were measured by both d.s.c. and optical methods. In the former, the samples were isothermally annealed in the sample holder at various temperatures for 4 to 5 min and then quickly quenched to room temperature before increasing the temperature at a scanning rate of 20°C min^{-1} in the DSC-7 to examine T_g behaviour. In the second procedure, films were covered with a glass slide and annealed on a hot stage at various constant temperatures around the phase separation temperature for a certain period of time. The phase separation temperature was taken as the lowest annealing temperature at which the film became cloudy.

The *PVT* properties were obtained using the Gnomix PVT apparatus by measuring the change in specific volume as a function of temperature. The density at 30°C and 1 atm was determined in a density gradient column. *Table 2* shows the equation-of-state characteristic parameters calculated for α-MSAN copolymers and a range of homopolymers. The characteristic parameters of α-MSAN copolymers were computed from homopolymer parameters for P(α-MS)[47] and PAN[14] using the mixing rules shown earlier.

RESULTS AND DISCUSSION

The open circles in *Figure 1* show the measured T_g for the α-MSAN copolymers synthesized; however, these points do not represent the typical plot for copolymers because the molecular weight of some copolymers was not high enough to correspond to the limiting value, T_g^∞. An estimate for T_g^∞ was made for each copolymer via equation (12) using the measured T_g and $\bar{M}_n$ assuming that $K = 1.27 \times 10^5$ determined for P(α-MS) applies for

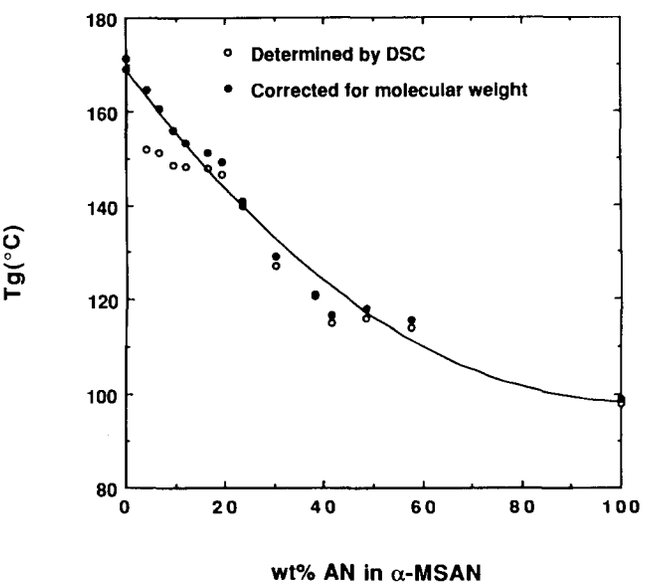

Figure 1 T_g for α-MSAN copolymers determined by d.s.c. (onset method) at 20°C min^{-1}: (○) experimental; (●) corrected for $\bar{M}_n$ using Fox relationship

Table 1 Polymers used in this study

Abbreviation	AN[a] (wt%) or polymer name	T_g(°C)	$\bar{M}_n$	$\bar{M}_w$[b]	Source
α-MSAN4	4.0	152	10070	17290	Monsanto
α-MSAN6.5	6.5	151	13520	22330	Monsanto
α-MSAN9.4	9.4	149	17260	28720	Monsanto
α-MSAN11.9	11.9	148	25420	40490	Monsanto
α-MSAN16.5	16.5	148	37840	65290	Monsanto
α-MSAN19.4	19.4	147	49200	90400	Monsanto
α-MSAN23.4	23.4	140	100300	179200	Monsanto
α-MSAN30	30.0	127	57000	160000	Luran KR 2566U (BASF)
α-MSAN38	38.1	121	81230	128800	Monsanto
α-MSAN41.4	41.4	115	75300	128400	Monsanto
α-MSAN48.5	48.5	116	62500	107000	Monsanto[c]
α-MSAN57.6	57.6	114	75000	116000	Monsanto[c]
SAN18	18.0	106	76100	172000	Monsanto
SAN20	20.0	106	88120	178000	Monsanto
SAN24	23.5	108	72070	160000	Monsanto
SAN26	26.0	106	57400	142400	Monsanto
SAN29	29.0	104	44000	276400	Monsanto
SAN30	30.0	105	168000	168000	Dow Chemical Co.
PMMA	Poly(methyl methacrylate)	108	52900	105400	Rohm & Haas V(811)100
PVC	Poly(vinyl chloride)	85	99000	213000	Diamond Shamrock Co.
TMPC	Tetramethylbisphenol A polycarbonate	190	–	33000	Bayer AG
PPO	Poly(2,6-dimethyl-1,4-phenylene oxide)	218	29400	39000	General Electric Co.
PCL	Poly(ε-caprolactone)	−74	15500	40400	Union Carbide Corp.
PC	Polycarbonate	127	4504	9900	Dow Chemical Co.
P(α-MS)	Poly(α-methylstyrene)	169	53398	55000	Polymer Laboratories Ltd

[a] Determined by elemental analysis
[b] Determined by g.p.c. based on polystyrene standards, except where noted
[c] Determined by laser light scattering by Monsanto

Table 2 Sanchez–Lacombe equation-of-state parameters[a]

	Temperature range 150–200°C			Temperature range 220–270°C		
Polymer	ρ^*(g cm^{-3})	P^*(bar)	T^*(K)	ρ^*(g cm^{-3})	P^*(bar)	T^*(K)
P(α-MS)	–	–	–	1.1268	4258	827
PAN[b]	1.2299	5357	853	1.2080	5192	909
α-MSAN6.5	1.1335	4329	829	1.1321	4319	833
α-MSAN9.42	1.1366	4362	829	1.1345	4346	835
α-MSAN11.9	1.1391	4389	830	1.1365	4369	837
α-MSAN16.45	1.1438	4439	831	1.1402	4412	841
α-MSAN19.4	1.1468	4471	832	1.1426	4439	843
α-MSAN23.4	1.1510	4515	833	1.1458	4477	846
α-MSAN30	1.1577	4588	835	1.1512	4538	852
α-MSAN41.4	1.1695	4713	838	1.1604	4645	861
PMMA	1.2601	5030	728	1.2564	5090	742
TMPC	–	–	–	1.1854	4395	729
PPO	–	–	–	1.1732	4083	758
PCL	–	–	–	1.1132	4212	736
PVC[c]	1.1461	5303	729	–	–	–

[a] Characteristic parameters obtained over the range of 0–50 MPa
[b] Obtained by linear extrapolation of copolymer parameters to 100% acrylonitrile[14]
[c] Obtained over the temperature range of 100–150°C[61]

each copolymer[48]:

$$T_g = T_g^{\infty} - K/\bar{M}_n \quad (12)$$

The full circles in *Figure 1* correspond to these corrected values, which define a more typical T_g plot for copolymers.

Blends of various homopolymers with α-MSAN copolymers were systematically examined for miscibility and phase separation temperatures when such *LCST* behaviour could be observed. These experimental data were used to calculate the interaction energy using the Sanchez–Lacombe equation-of-state theory. The analysis assumes that the experimental phase separation temperatures are adequately represented by the spinodal curve and that the 'bare' interaction energy density ΔP^* is independent of temperature. The latter means that any temperature dependence of the Flory–Huggins parameter $B(T)$ stems entirely from compressibility effects[49]. Where possible, ΔP^* was determined as a function of copolymer composition and, by fitting these results to equation (9), ΔP_{ij}^* values for each repeating unit pair could be obtained. The ΔP_{ij}^* values obtained for blends of the various homopolymers with α-MSAN copolymers were then compared with corresponding ones obtained from SAN copolymers whenever possible. Flory–Huggins B_{ij} values were also calculated from the experimental miscibility limits using the binary interaction model for comparison with the ΔP_{ij}^* values.

Blends with PMMA

Suess *et al.*[38] studied blends of α-MSAN copolymers ($\bar{M}_w$ ranging from 5900 to 160 000) with PMMA ($\bar{M}_w = 43\,000$). Clear films were obtained from 18.5 to 41.3 wt% AN in α-MSAN. Phase separation temperatures were reported where the AN content in the copolymer was in the range from 31.3 to 44.3 wt%, while in the range from 18.5 to 30.5 wt% AN, the phase separation temperatures were apparently above the thermal decomposition temperature. Goh *et al.*[20] reported the cloud points for blends of a commercial α-MSAN containing 30 wt% AN with atactic and isotactic PMMA.

In this work, PMMA was blended with the poly(α-methylstyrene) (P(α-MS)) and α-MSAN copolymers of different AN contents (see *Table 1* for details of these polymers) at 50 wt% PMMA, close to the critical point for these blends. Blend films prepared by hot casting were transparent and exhibited a single composition-dependent T_g, as expected for miscible blends, for a wide range of α-MSAN copolymers. As an example, *Figure 2* shows the T_g dependence of blends of PMMA with α-MSAN9.4 and α-MSAN30. Cloudy films were obtained when PMMA was blended with P(α-MS) and α-MSAN copolymers containing 38.1 wt% AN and higher, indicating immiscibility. Two T_g values were observed for the former blend; but for the latter mixtures, two T_g values could not be observed since the component T_g values are too similar to resolve by d.s.c. *Figure 3* shows the experimental *LCST*-type phase separation temperatures for blends of PMMA with α-MSAN9.4 and α-MSAN30, determined from visual cloud-point behaviour. Blends of PMMA with α-MSAN6.5 and α-MSAN11.9 were annealed below the cloud point for a day at 180 and 200°C, respectively. After this treatment, the samples were transparent and d.s.c. thermograms showed single T_g behaviour. This indicates that the observed phase separation can be reversed, which assures that the cloud points determined represent an equilibrium phase boundary.

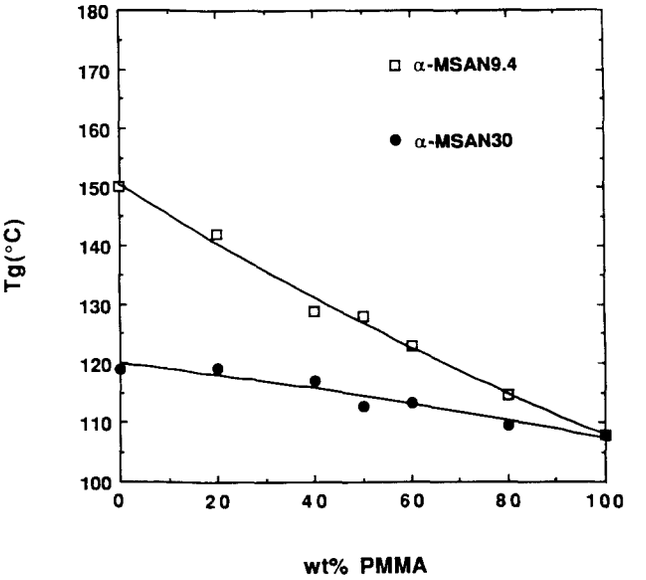

Figure 2 T_g (defined by onset method) behaviour of PMMA blends with selected α-MSAN copolymers determined by d.s.c. at 20°C min^{-1}

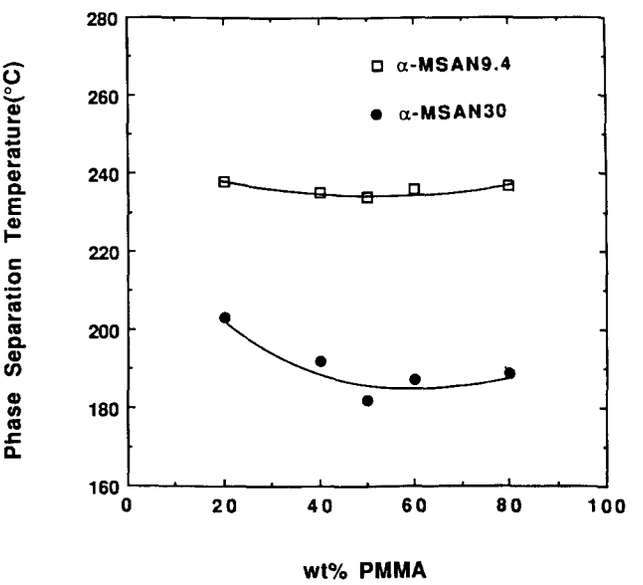

Figure 3 Phase separation temperatures of PMMA blends with selected α-MSAN copolymers determined by d.s.c.

Experimentally determined phase separation temperatures for blends of 50 wt% PMMA with α-MSAN copolymers are shown by the full circles in *Figure 4a*. The open circles denote blends that were phase separated as prepared; hence, the actual phase separation temperature must lie below the drying temperature of 150°C as denoted by the arrows. From these observations, we can conclude that below 150°C PMMA forms miscible blends with α-MSAN copolymers from 4 to 30 wt% AN. The phase separation temperatures shown in *Figure 4a* plus the characteristic parameters of α-MSAN copolymers given in *Table 2* were used to calculate, via equation (10), the ΔP^* values shown by the full circles in *Figure 4b*. Equation (7) can be fitted to the latter points to obtain all these ΔP_{ij}^* values ($\Delta P^*_{\alpha\text{-MS/AN}} = 7.87$, $\Delta P^*_{\alpha\text{-MS/MMA}} = 0.02$ and $\Delta P^*_{\text{MMA/AN}} = 5.06\,\text{cal cm}^{-3}$); however, it is believed that more reliable values are obtained by reducing the degrees of freedom in the fitting process. Setting

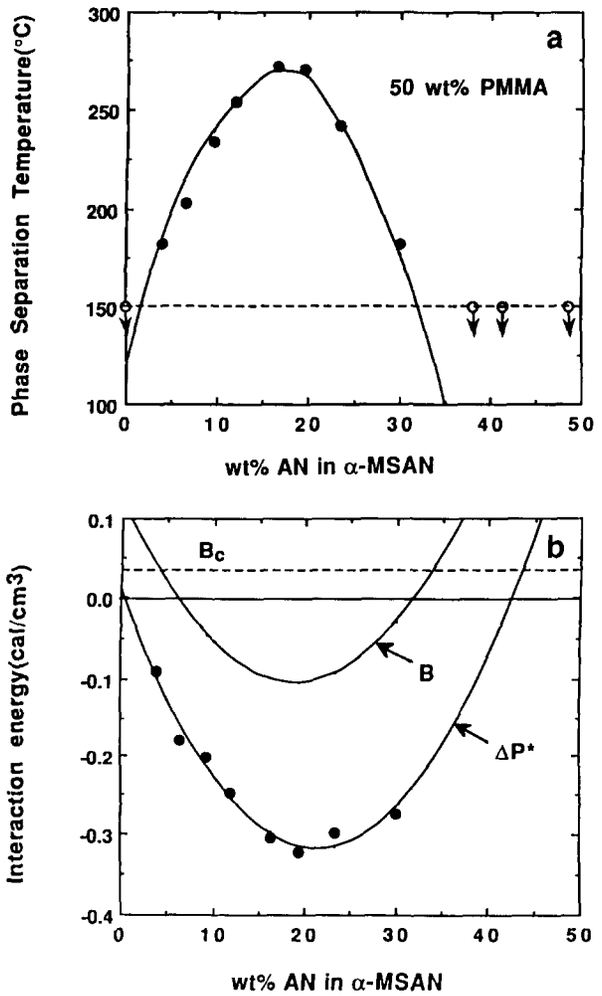

Figure 4 (a) Phase separation temperatures and (b) bare interaction parameters for 50/50 PMMA/α-MSAN blends. The broken line in (a) represents the blend drying temperature. The full curve in (a) is the estimated spinodal temperature using equation (9) for ΔP^*, while the full circles are the experimentally determined phase separation temperatures. Arrows on the open circles correspond to blends with phase separation temperatures below the drying temperature. The full curves in (b) are interaction energies calculated from the predicted B_{ij} and ΔP^*_{ij} values (see text), while full circles are the ΔP^* determined from the experimental phase diagram using the lattice-fluid theory

$\Delta P^*_{\alpha\text{-MS/AN}} = 8.59\,\text{cal cm}^{-3}$ (obtained from blends of TMPC and α-MSAN copolymer, discussed in the next section) and obtaining the remaining two parameters by fitting leads to $\Delta P^*_{\alpha\text{-MS/MMA}} = 0.02$ and $\Delta P^*_{\text{MMA/AN}} = 4.36\,\text{cal cm}^{-3}$, which is a more reasonable set when all available systems are considered. The full curves in *Figure 4b* were calculated from this latter set of ΔP^*_{ij}. The recommended set of ΔP^*_{ij} represent the data points in *Figures 4a* and *4b* essentially as well as the set obtained without fixing $\Delta P^*_{\alpha\text{-MS/AN}}$. Note that $\Delta P^*_{\alpha\text{-MS/AN}}$ is relatively large, as observed[14] for $\Delta P^*_{\text{S/AN}}$. The full curve in *Figure 4a* represents the spinodal estimated from the ΔP^*_{ij} calculated earlier. The estimated spinodal curve and the experimental phase separation temperatures coincide very well. In addition, the region of copolymer compositions that form miscible and immiscible blends, represented by the full and open circles, respectively, are bounded by the spinodal curve quite well. Note that blends of PMMA with some α-MSAN copolymers are not miscible even though ΔP^* is negative because of the sizeable equation-of-state contributions for these blends.

The same method of interaction energy analysis was also performed for blends of PMMA/α-MSAN at 40/60 and 60/40 (weight ratios). The ΔP^*_{ij} predicted at these different compositions were close to that obtained at 50/50 (close to the critical point). Therefore, interaction energy analysis for blend systems after this were evaluated at 50/50 or near the critical point.

A better understanding of the issues responsible for the observed phase behaviour of blends of PMMA with α-MSAN can be seen by a closer examination using equation (11). In the following, α-MSAN copolymers are designated as component 1 and PMMA as component 2. Of course, these blends are miscible because of the negative ΔP^* over the range of AN contents shown in *Figure 4b*, and a dominant factor in this is the strong intramolecular repulsion between α-MS and AN units. However, compressibility or equation-of-state effects play a role. As the AN content in α-MSAN copolymers increases, T_1^* and $\tilde{\rho}_1$ become larger, as shown in *Table 2*. The smaller compressibility of α-MSAN copolymers caused by $\tilde{\rho}_1$ increasing is favourable for phase stability. However, as the AN content goes up, $(T_1^* - T_2^*)^2$ increases, which strongly decreases blend stability. Therefore, as AN content increases, there is competition among these terms, which leads to immiscibility at higher contents of AN in α-MSAN.

The interaction energies ΔP^* or ΔP^*_{ij} deduced from the above analysis can be converted into the corresponding quantities B or B_{ij} in the Flory–Huggins theory as shown by Kim and Paul[15]:

$$B_{sc} = \tilde{\rho}\Delta P^* + \left[P_2^* - P_1^* + (\phi_2 - \phi_1)\Delta P^* + \frac{RT}{\tilde{\rho}}\left(\frac{1}{r_1^o v_1^*} - \frac{1}{r_2^o v_2^*}\right) - RT\left(\frac{\ln(1-\tilde{\rho})}{\tilde{\rho}^2} + \frac{1}{\tilde{\rho}}\right)\left(\frac{1}{v_1^*} - \frac{2}{v_2^*}\right)\right]^2 \Bigg/ \left[\frac{2RT}{v^*}\left(\frac{2\ln(1-\tilde{\rho})}{\tilde{\rho}^3} + \frac{1}{\tilde{\rho}^2(1-\tilde{\rho})} + \frac{(1-1/r)}{\tilde{\rho}^2}\right)\right] \quad (13)$$

The interaction energy densities at the drying temperature of 150°C from the above ΔP^*_{ij} values are $B_{\alpha\text{-MS/MMA}} = 0.12$, $B_{\text{MMA/AN}} = 4.32$ and $B_{\alpha\text{-MS/AN}} = 7.96\,\text{cal cm}^{-3}$. Note that $B_{\text{MMA/AN}}$ calculated above is close to $4.11\,\text{cal cm}^{-3}$, reported by Nishimoto *et al.*[1]. The larger values of B_{ij} compared to ΔP^*_{ij} reflect the effect of equation-of-state contributions. The curve designated as B in *Figure 4b*, computed from the B_{ij} values at 150°C, matches the experimental miscibility limits very well.

It is interesting to compare the phase behaviour of PMMA blends with α-MSAN copolymers to the similar blends with SAN copolymers and the corresponding ΔP^*_{ij} deduced. The phase behaviour of blends of PMMA with SAN copolymers[1,6,16,27,50–54] has been documented extensively. Here, the results of Fowler *et al.*[27] (PMMA $\bar{M}_w = 105\,400$) and Kressler *et al.*[16] (PMMA $\bar{M}_w = 43\,000$) will be analysed separately. The SAN copolymers used in these two cases have $\bar{M}_w$ above 160 000. Blends of lower-molecular-weight polymers have higher phase separation temperatures. Therefore, the molecular-weight effect has to be taken into account in the interaction energy calculations. The bare interaction energies calculated for these two blends with different molecular

weights will be analysed separately before any quadratic fitting is performed to obtain the ΔP^*_{ij} values.

Fowler *et al.*[27] reported that PMMA is miscible with SAN copolymers containing about 9.5 to 28 wt% AN. Miscible blends with SAN copolymers containing 25 wt% AN or less exhibit phase separation at temperatures above thermal decomposition of these materials. Phase separation temperatures were reported for only two SAN copolymers, SAN25 and SAN28, that can reliably be used for the current quantitative analysis. To aid this analysis, phase separation temperatures were determined here for blends of the same PMMA with SAN26, SAN29 and SAN30 (molecular-weight information listed in *Table 1*). The phase separation temperatures obtained here and by Fowler *et al.*, represented by the full circles in *Figure 5a*, are combined for this analysis. The open circles refer to immiscible blends. The full and open squares in *Figure 5a* correspond to miscible and immiscible blends reported by Kressler *et al.*[16] for PMMA with $\bar{M}_w = 43\,000$. The upper limits of AN contents for PMMA miscibility with α-methylstyrene and styrene copolymers are about the same. However, for SAN copolymers, miscibility is limited to a more narrow range for low AN contents. In the miscible range, SAN blends show much higher phase separation temperatures than do α-MSAN blends. The fact that most of the available range does not lead to measurable phase separation temperatures limits the extent of the ΔP^* analysis.

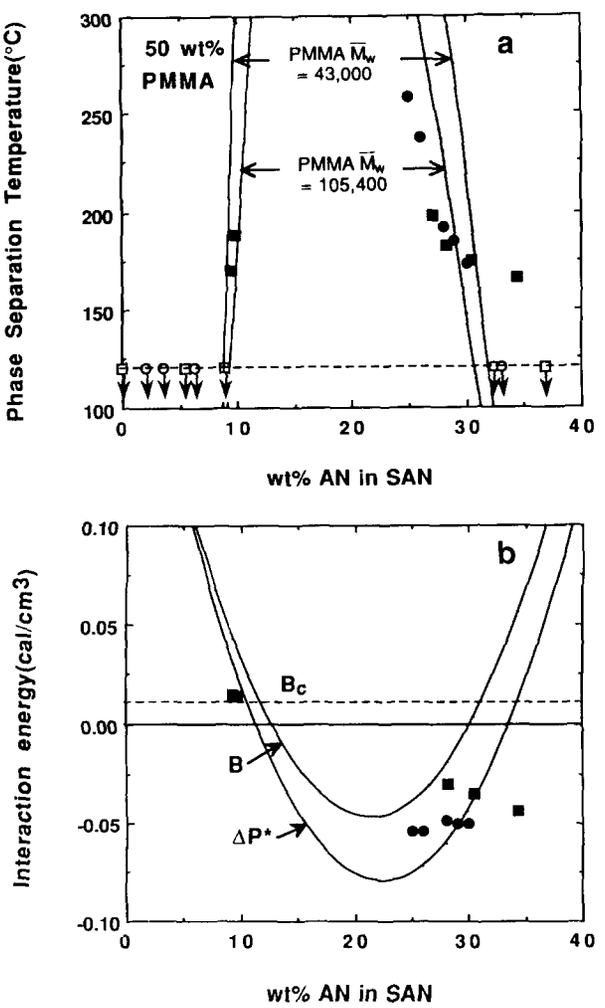

Figure 5 (a) Phase separation temperatures and (b) bare interaction parameters for 50/50 PMMA/SAN blends. Miscible and immiscible blends of PMMA ($\bar{M}_w = 105\,400$) with SAN[27] are represented by the full and open circles, respectively, while the miscible and immiscible blends of PMMA ($\bar{M}_w = 43\,000$) with SAN[16] are represented by the full and open squares, respectively. The broken line in (a) represents the blend drying temperature. The inner and outer lines in (a) are the estimated spinodal temperatures for blends with PMMA ($\bar{M}_w = 105\,400$) and blends with PMMA ($\bar{M}_w = 43\,000$), respectively, using equation (9) for ΔP^*, while the full circles and squares are the experimentally determined phase separation temperatures. Arrows beside the open circles and squares correspond to blends with phase separation temperatures below the drying temperature. The full curves in (b) are the interaction energies calculated from the predicted B_{ij} and ΔP^*_{ij} values, while full circles and squares are the ΔP^* values determined from the experimental phase diagram for blends of PMMA ($\bar{M}_w = 105\,400$) and blends with PMMA ($\bar{M}_w = 43\,000$) using the lattice-fluid theory

As noted earlier, somewhat different characteristic parameters are obtained depending on the temperature range over which *PVT* data are fitted to equation (6). The phase separation temperatures in *Figure 5a* fall primarily within the 150–200°C range, so, for consistency, the values from *Table 2* for this range were used in these calculations. *Figure 5b* shows the values of ΔP^* calculated from the data in *Figure 5a* using the Sanchez–Lacombe theory with the various assumptions mentioned earlier. Because the phase separation temperatures exceed the decomposition temperature over a large portion of the AN composition range when miscibility occurs, these results are too sparse to expect a fitting of equation (9) to give a meaningful set of all the ΔP^*_{ij} values. As an alternative, we set the S/AN interaction at the value of 7.37 cal cm^{-3} as determined by Kim *et al.*[14] (from blends of TMPC with SAN copolymers) and use the fitting to deduce $\Delta P^*_{S/MMA} = 0.23$ and $\Delta P^*_{MMA/AN} = 4.52$ cal cm^{-3}. The inner and outer lines in *Figure 5a* represent the spinodal lines calculated for the two PMMA $\bar{M}_w$ using the above set of ΔP^*_{ij}. These lines seem to match the miscibility limits and phase separation temperatures for the corresponding blends relatively well. The arrows on the open circles and squares indicate that the phase separation temperatures for these blends lie below the drying temperature of 120°C. Note that the $\Delta P^*_{S/MMA}$ calculated here (0.23 cal cm^{-3}) is similar to the $\Delta P^*_{S/MMA}$ calculated using the critical molecular-weight information for oligomeric blends of PMMA with polystyrene (0.30 to 0.36 cal cm^{-3})[55]. In addition, a reanalysis of recent results for blends of TMPC and SMMA[47] showed that $\Delta P^*_{S/MMA} = 0.25$ cal cm^{-3}. The MMA/AN interaction deduced (4.52 cal cm^{-3}) is close to the value extracted from the data for blends of PMMA with α-MSAN copolymers (4.36 cal cm^{-3}).

The Flory–Huggins interaction energy densities B_{ij} calculated at the drying temperature of 120°C from the above ΔP^*_{ij} are $B_{S/MMA} = 0.23$, $B_{MMA/AN} = 4.49$ and $B_{S/AN} = 7.02$ cal cm^{-3}, respectively. The B_{ij} values so obtained are close to those reported by Nishimoto *et al.*[1]. The curve labelled *B* in *Figure 5b* shows the interaction energies calculated from the B_{ij} for PMMA/SAN blends at 120°C.

In summary, replacing α-methylstyrene for styrene in AN copolymers broadens the miscibility window for blends with PMMA but lowers the phase separation temperatures at mid AN range, as shown in *Figures 4a* and *5a*. The change in phase behaviour observed is due to changes in ΔP^*_{ij} and ΔT^*_{ij}. As shown later in *Table 4*, $\Delta P^*_{\alpha\text{-MS/AN}}$ is greater than $\Delta P^*_{S/AN}$. However, $\Delta P^*_{\alpha\text{-MS/MMA}}$ is smaller than $\Delta P^*_{S/MMA}$. The values of $\Delta P^*_{MMA/AN}$ calculated from the two series are in good agreement with each other. A significant difference in the equation-of-state

contribution occurs when α-methylstyrene replaces styrene in the AN copolymer. This may be seen by comparing $T^*_{\alpha\text{-MS/MMA}} = 85°C$ *versus* $T^*_{S/MMA} = 23°C$ (where $\Delta T^*_{ij} = T_i^* - T_j^*$). These two factors, ΔP^*_{ij} and ΔT^*_{ij}, are the primary terms that govern blend phase behaviour, as may be seen from equation (11).

Blends with TMPC

Blends of tetramethyl bisphenol-A polycarbonate (TMPC) with α-MSAN copolymers were prepared by precipitation from tetrahydrofuran (THF) into methanol. Blends with a single T_g (see, for example, *Figure 6*) were observed for α-MSAN copolymers containing 4 to 16.5 wt%, while two glass transitions were found for copolymers containing 19.4 to 30 wt% AN and for P(α-MS) ($\bar{M}_w = 55\,000$). Phase separation temperatures were determined by examining the T_g behaviour of blends annealed 4 to 5 min at various temperatures as described by Kim *et al.*[14]. Phase-separated blends based on α-MSAN copolymers containing 9.4 to 16.5 wt% AN became homogeneous again when annealed at 170°C for 2 days. This demonstration of reversibility proves that the observed phase separation reflects equilibrium *LCST*[36,56–60]. Blends based on α-MSAN4 and α-MSAN6.5 did not become homogeneous after the same thermal treatment, most probably because of kinetic factors.

The full circles in *Figure 7a* indicate the 50/50 blends found to be miscible at 180°C, while the open circles indicate blends that are immiscible. Using these measured phase separation temperatures and the characteristic parameters listed in *Table 2*, the ΔP^* values shown in *Figure 7b* were calculated. Since there are only three points in *Figure 7b*, a quadratic fit to obtain all three ΔP^*_{ij} was not attempted. Instead, we set $\Delta P^*_{TMPC/AN} = 5.92\ cal\ cm^{-3}$ based on the results for blends of TMPC with SAN[14] and deduce only the remaining two from fitting of the model to these data, i.e. $\Delta P^*_{\alpha\text{-MS/TMPC}} = 0.005$ and $\Delta P^*_{\alpha\text{-MS/AN}} = 8.59\ cal\ cm^{-3}$. The full curve in *Figure 7a* represents the spinodal estimated from these ΔP^*_{ij}. Note that TMPC is not miscible with α-MSAN copolymers containing 17 to 18 wt% AN, even though the calculated ΔP^* has relatively large negative values up to about 25 wt% AN. This is the result of the large $(T_1^* - T_2^*)$, which grows with AN content.

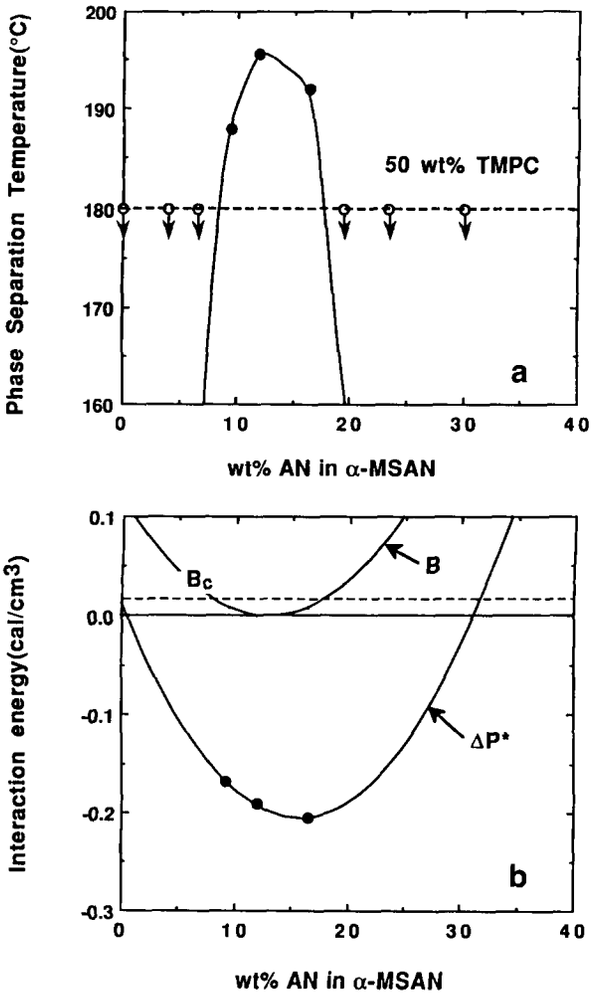

Figure 7 (a) Phase separation temperatures and (b) bare interaction parameters for 50/50 TMPC/α-MSAN blends. The broken line in (a) represents the blend drying temperature. The full curve in (a) shows the estimated spinodal temperatures using equation (9) for ΔP^*, while the full circles are the experimentally determined phase separation temperatures. Arrows on the open circles correspond to blends with phase separation temperatures below the drying temperature. The full curves in (b) show the interaction energies calculated from the predicted B_{ij} and ΔP^*_{ij} values, while the full circles are the ΔP^* values determined from the experimental phase diagram using the lattice-fluid theory

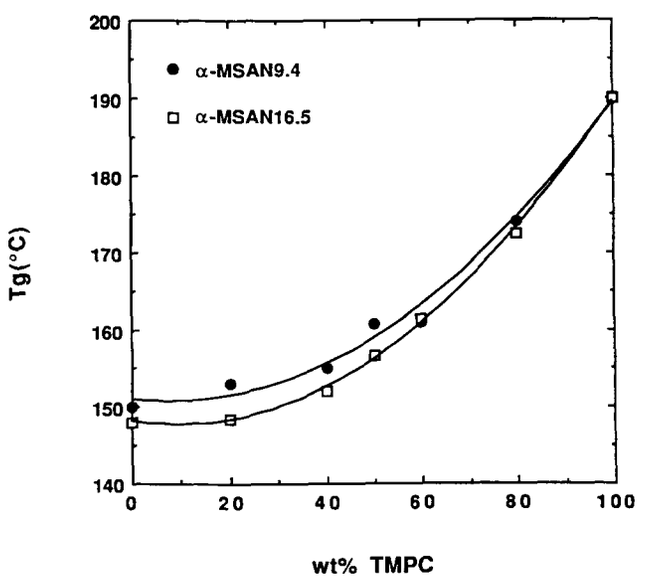

Figure 6 T_g (defined by onset method) behaviour of TMPC blends with selected α-MSAN copolymers determined by d.s.c. at 20°C min^{-1}

The Flory–Huggins interaction energy densities calculated from the above ΔP^*_{ij} at the drying temperature of 180°C are $B_{\alpha\text{-MS/TMPC}} = 0.18$, $B_{TMPC/AN} = 5.67$ and $B_{\alpha\text{-MS/AN}} = 7.84\ cal\ cm^{-3}$. The curve designated as B in *Figure 7b* shows the interaction energies calculated from the B_{ij} for TMPC/α-MS/AN blends at 180°C. B_{ij} and ΔP^*_{ij} values deduced here may be compared to those obtained for TMPC/SAN blends found by Kim *et al.*[14] in *Table 4*.

The use of α-methylstyrene in place of styrene in AN copolymers decreases the width of the miscibility window and lowers the phase separation temperatures for blends with TMPC, as seen in *Figure 8*, because of differences in ΔP^*_{ij} and ΔT^*_{ij}. *Figure 8* is plotted for blends of TMPC with SAN and α-MS/AN copolymers at their respective $\bar{M}_w$. However, calculations show that, if the molecular weights of the α-MS/AN copolymers were similar to those

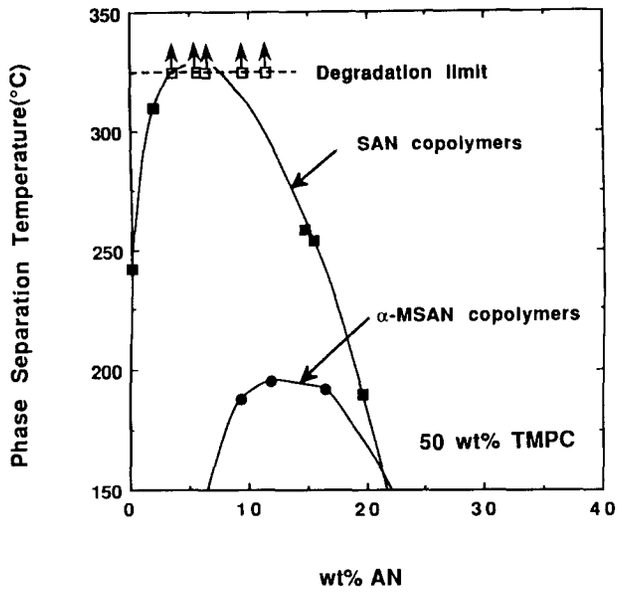

Figure 8 Phase separation temperatures for 50/50 blends of TMPC with α-MSAN copolymers (●) and SAN copolymers (■). Arrows on the open squares correspond to blends of TMPC with SAN where the phase separation temperatures are above the degradation limit for the blends

of SAN copolymers, slightly lower phase separation temperatures (about 15 to 20°C) should be observed, as expected. Again, the α-MS/AN energy interaction is more repulsive than that of the S/AN pair, while the interaction energy for the α-MS/TMPC pair is a small positive value rather than the small negative value for the S/TMPC pair. With regard to the latter, note that blends of polystyrene and TMPC are miscible[15], while blends of P(α-MS) ($\bar{M}_w = 55\,000$) and TMPC are immiscible. In addition, the $\Delta T^*_{\alpha\text{-MS/TMPC}} = 98°C$ is somewhat greater than the $\Delta T^*_{S/TMPC} = 81°C$, both calculated for the temperature range where the phase separation temperature occurs. These two factors combined alter the phase behaviour for blends with TMPC. The interaction energy is the dominant factor that lowers the phase separation temperatures and narrows the miscibility boundaries for TMPC blends with α-MSAN copolymers compared to SAN copolymers.

Blends with PVC

Kim *et al.*[29] found that blends of α-MSAN30 with PVC showed a single T_g for all compositions and that phase separation on heating does not occur prior to 250°C, which is beyond the normal processing range for PVC. Since blends of α-MSAN copolymers with PVC are useful to improve the heat resistance of PVC, the miscibility behaviour for copolymers with other AN contents were examined in this work. The blends were prepared by precipitation from THF solution into methanol. Single glass transitions were observed for α-MSAN copolymers containing from 11.9 to 30 wt% AN (see, for example, *Figure 9*). However, two T_g values were found for blends of PVC with α-MSAN copolymers containing AN levels of 9.4 wt% or less and 38.1 wt% or higher. PVC blends with α-MSAN11.9 and α-MSAN16.5 that had phase separated on heating gave a single T_g by d.s.c. scan after annealing at 130°C for 2 days. This demonstrates that the observed phase separation is reversible; however, owing to the poor thermal stability of PVC, it was not feasible to test reversibility at higher temperatures.

The full circles in *Figure 10a* represent the phase separation temperatures observed using the d.s.c. method for miscible blends. The open circles denote immiscible blends, which evidently have phase separation temperatures below 130°C. Characteristic equation-of-state parameters for PVC were obtained from *PVT* data over the temperature range from 100 to 150°C[61]. Using the characteristic equation-of-state parameters listed in *Table 2* and the observed phase separation temperatures, the ΔP^* values calculated are shown in *Figure 10b*. Quadratic fitting of equation (9) to the latter gives $\Delta P^*_{\alpha\text{-MS/VC}} = 0.26$, $\Delta P^*_{VC/AN} = 4.30$ and $\Delta P^*_{\alpha\text{-MS/AN}} = 8.60\,cal\,cm^{-3}$. Note that the $\Delta P^*_{\alpha\text{-MS/AN}}$ deduced from this system is essentially identical to the value of $8.59\,cal\,cm^{-3}$ obtained from blends of TMPC with α-MSAN copolymers. This serves as a useful check on the universality of the interaction energy for α-MS/AN from one system to another. The full curve in *Figure 10a* is the locus of spinodal temperatures calculated from these ΔP^*_{ij} values, and it represents the experimental phase behaviour rather well. PVC is immiscible with α-MSAN copolymers when the AN content is lower than 11.9 wt% and higher than 41.4 wt% since the estimated phase separation temperatures for these blends are below 130°C. An important factor contributing to the immiscibility of PVC at higher AN contents is the growth in the ΔT^* term. The Flory-Huggins B_{ij} values at 130°C computed from these ΔP^*_{ij} are $B_{\alpha\text{-MS/VC}} = 0.37$, $B_{VC/AN} = 4.22$ and $B_{\alpha\text{-MS/AN}} = 8.04\,cal\,cm^{-3}$. The resulting curve for B is shown in *Figure 10b*.

Blends of PVC with SAN copolymers have been examined extensively[30,62-64]. Kim *et al.* reported that PVC is miscible with SAN copolymers containing AN from 11.5 to 28 wt% AN[30]. Visual cloud points reported for these blends range from 175 to 193°C. Since calculation of interaction energies requires accurate phase separation temperatures, these blends were re-examined using the careful d.s.c. and optical methods employed in this work. For the d.s.c. method, the blends were precipitated from THF into methanol and dried at 100°C for 2 days. For the optical method, blend solutions based on methyl ethyl ketone were sandwiched

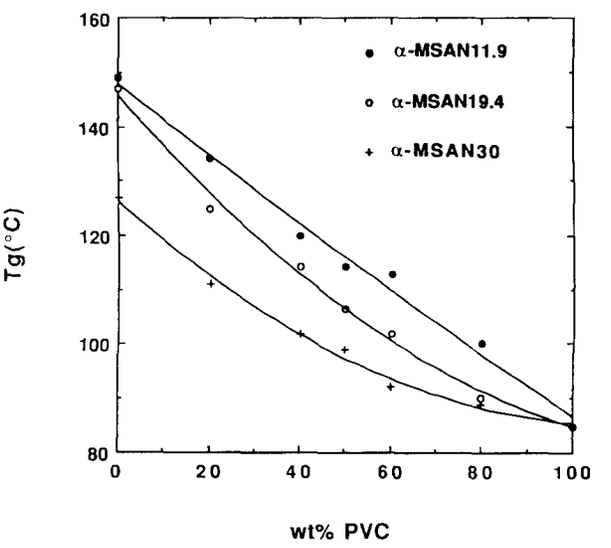

Figure 9 T_g (defined by onset method) behaviour of PVC blends with selected α-MSAN copolymers determined by d.s.c. at 20°C min^{-1}

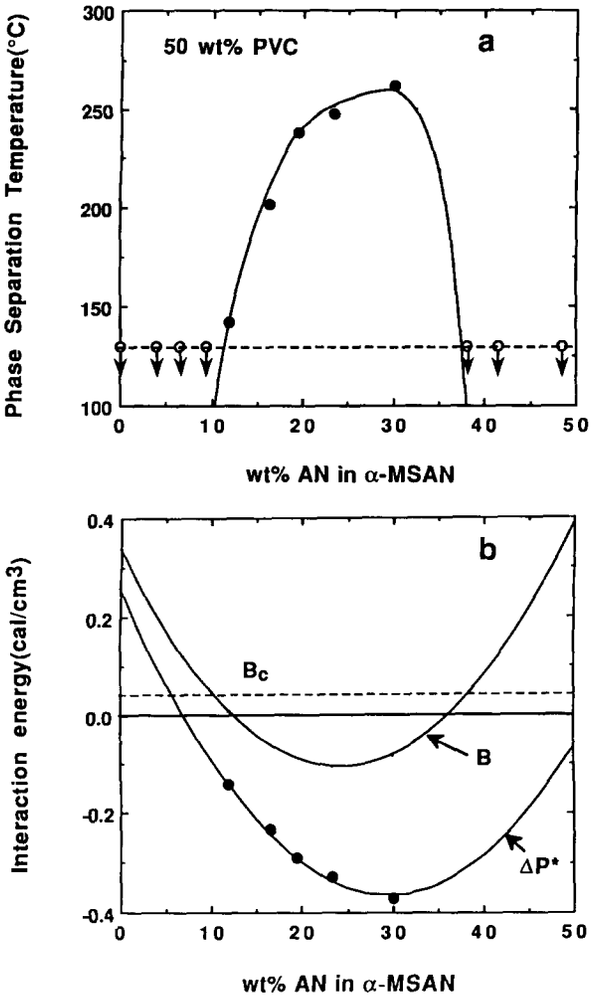

Figure 10 (a) Phase separation temperatures and (b) bare interaction parameters for 50/50 PVC/α-MSAN blends. The broken line in (a) represents the blend drying temperature. The full curve in (a) shows the estimated spinodal temperatures using equation (9) for ΔP^*, while the full circles are the experimentally determined phase separation temperatures. Arrows on the open circles correspond to blends with phase separation temperatures below the drying temperature. The full curves in (b) show the interaction energies calculated from the predicted B_{ij} and ΔP^*_{ij} values, while the full circles are the ΔP^* determined from the experimental phase diagram using the lattice-fluid theory

between two glass slides and heated to 60°C, before further drying in the vacuum oven at 100°C for 2 days. To limit thermal dehydrochlorination of PVC, 1 to 3 wt% of lead-based stabilizer (Halstab 30 from Hammond Lead Products Inc.) was added. The blends with stabilizer showed the same phase behaviour as that obtained from blends without stabilizer. The full circles in *Figure 11a* refer to phase separation temperatures obtained using the d.s.c. method; those obtained via the optical method were about 5 to 10°C higher. The open circles denote blends found to be immiscible at 100°C. All phase separation temperatures obtained here are lower than those reported by Kim *et al.*[30]. It is believed that the d.s.c. method is more accurate than the optical approach, since it is sometimes difficult to define the point at which a blend first turns cloudy owing to PVC degradation. Moreover, rate effects may become a factor especially when continuous heating of the sample is used. It is also important to be certain that lowering the temperature will in fact reverse the phase separation produced on heating in order to verify that this is an equilibrium phase diagram. Blends with SAN copolymers containing 15.5 and 19.5 wt% AN that had been heated above the phase separation temperature become one-phase again after annealing at 110°C for a day.

Using the characteristic equation-of-state parameters from *Table 2* and the d.s.c. phase separation temperatures from *Figure 11a*, the ΔP^* values shown by the full circles in *Figure 11b* were calculated for the miscible blends. These values are extremely small in magnitude, which causes equation-of-state to dominate. To illustrate this, the open circles in *Figure 11b* were computed for compositions outside the miscibility region assuming a phase separation temperature of 100°C (the actual ΔP^* must lie above this as denoted by the arrows on each point). The open and full circles fall more or less on one curve, which indicates the insensitivity of the ΔP^* calculated to the phase separation temperature. On the other hand, the predicted phase separation temperature

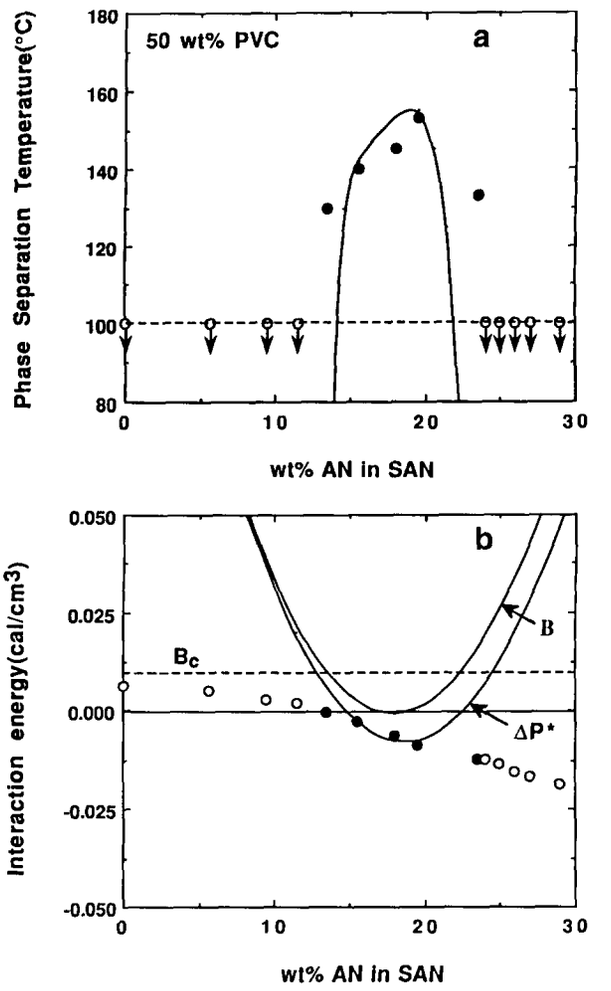

Figure 11 (a) Phase separation temperatures and (b) bare interaction parameters for 50/50 PVC/SAN blends. The broken line in (a) represents the blend drying temperature. Miscible and immiscible blends are represented by the full and open circles, respectively. The full curve in (a) shows the estimated spinodal temperatures using equation (9) for ΔP^*, while the full circles are the experimentally determined phase separation temperatures. Arrows on the open circles correspond to blends with phase separation temperatures below the drying temperature. The full curves in (b) show the interaction energies calculated from the predicted B_{ij} and ΔP^*_{ij} values, while full circles are the ΔP^* determined from the experimental phase diagram using the lattice-fluid theory. The open circles in (b) refer to ΔP^* calculated for the immiscible blends using the drying temperature as the phase separation temperature

is extremely sensitive to the ΔP^* used. These facts severely limit the ΔP^*_{ij} information that can be extracted from observations on this system. If we set $\Delta P^*_{VC/AN} = 4.30$ (from the PVC/α-MSAN system) and $\Delta P^*_{S/AN} = 7.37\,cal\,cm^{-3}$ (from the TMPC/SAN system), then the curves 1–4 in *Figure 12* can be generated using the various choices for $\Delta P^*_{S/VC}$ shown. Curve 4 probably best represents the magnitude of the ΔP^* values; however, it is shifted to the right and this ΔP^*_{ij} set does not lead to a spinodal prediction that reasonably represents the phase separation temperature observed. However, by setting $\Delta P^*_{VC/AN} = 4.30\,cal\,cm^{-3}$ and simultaneously solving equation (9) for blends based on SAN copolymers containing 15.5 and 19.5 wt% AN gave $\Delta P^*_{S/VC} = 0.17$ and $\Delta P^*_{S/AN} = 6.26\,cal\,cm^{-3}$. This ΔP^*_{ij} set leads to curve 5 in *Figure 12* and predicts a spinodal line (see *Figure 11a*) that better represents the experimental phase separation temperatures; however, the miscibility limits predicted are too narrow. We believe that the value $\Delta P^*_{S/AN} = 7.37\,cal\,cm^{-3}$ is more realistic since it better represents other systems (e.g. PMMA/SAN system). For the PVC/SAN system, it does not seem possible to obtain a single set of interaction energies that represent the ΔP^* values and map both the phase separation temperatures and the miscibility limits well. Because of this, the best we can conclude about the value of $\Delta P^*_{S/VC}$ is that it is small, perhaps in the range of 0.15 to $0.4\,cal\,cm^{-3}$. The B_{ij} values that correspond to the ΔP^*_{ij} set corresponding to curve 5 in *Figure 12* are $B_{S/VC} = 0.16$, $B_{VC/AN} = 5.60$ and $B_{S/AN} = 6.08\,cal\,cm^{-3}$. The values of B computed from these parameters are also shown in *Figure 11b*.

From *Figure 13*, we can see that the use of α-methylstyrene in place of styrene in AN copolymers

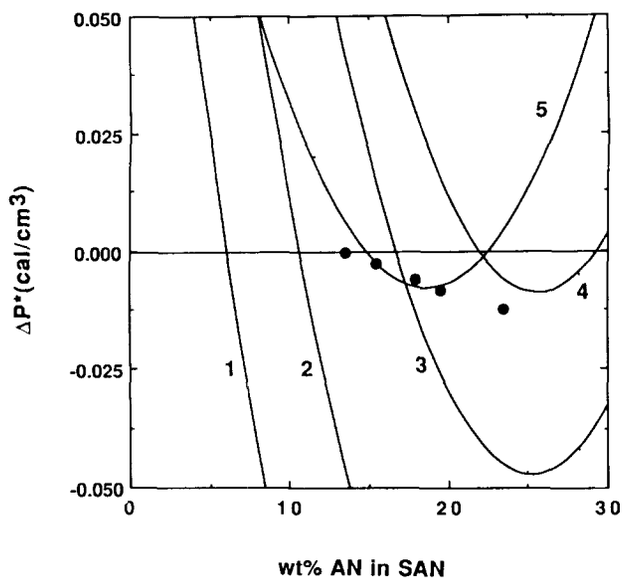

Figure 12 Bare interaction energies for blends of 50/50 PVC/SAN, calculated from phase separation temperatures determined by d.s.c. The full curves were calculated from equation (9) using the various sets of ΔP^*_{ij} ($cal\,cm^{-3}$) shown below:

Curve	$\Delta P^*_{S/VC}$	$\Delta P^*_{VC/AN}$	$\Delta P^*_{S/AN}$
1	0.15	4.30	7.37
2	0.25	4.30	7.37
3	0.30	4.30	7.37
4	0.40	4.30	7.37
5	0.17	4.30	6.26

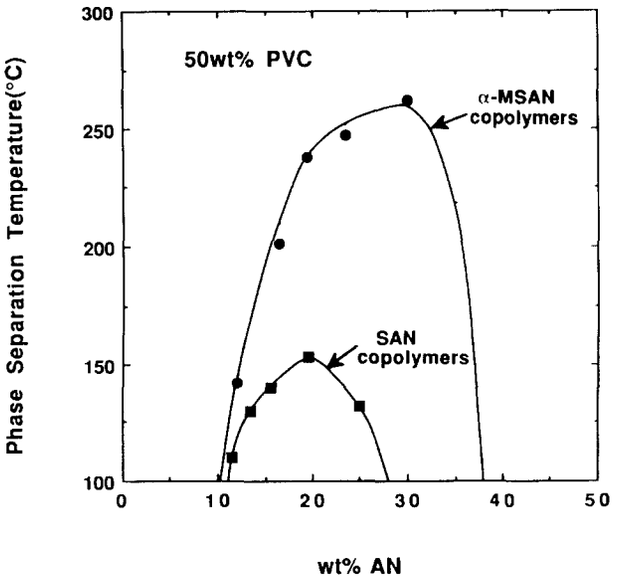

Figure 13 Comparison of phase separation temperatures for blends of PVC with α-MSAN copolymers (●) and SAN copolymers (■)

broadens the miscibility window and increases the phase separation temperature. While analogue calorimetry results suggest that α-MS interacts more favourably with PVC than does styrene[30], the $\Delta P^*_{\alpha\text{-MS/VC}}$ and $\Delta P^*_{S/VC}$ reported here do not differ much. The magnitude of the repulsive interaction between α-MS and AN is greater than that between S and AN units. However, the dominant factor that alters the phase behaviour is the difference in characteristic temperatures, i.e. $\Delta T^*_{\alpha\text{-MC/VC}} = 91°C$ *versus* $\Delta T^*_{S/VC} = 15°C$.

Blends with PPO

It is well known that poly(2,6-dimethyl-1,4-phenylene oxide) (PPO) and polystyrene are miscible and do not phase separate on heating prior to decomposition of the components[65–68]. Therefore, the interaction energy for PPO/PS cannot be calculated using the approach employed above. However, if we assume that the phase separation temperature for PPO/PS is greater than 320°C, then, using the characteristic parameters listed in *Table 4*, $\Delta P^*_{S/PPO}$ must be less than $-0.05\,cal\,cm^{-3}$.

PPO ($\bar{M}_w = 39\,000$) is also miscible with P(α-MS), but these blends do phase separate on heating. *Figure 14* shows the T_g behaviour for blends prepared by hot casting from trichloroethylene and dried at 220°C. *Figure 15a* shows the phase separation temperature for blends of PPO with P(α-MS). From the phase separation temperatures in *Figure 15a* and the characteristic parameters listed in *Table 2*, the ΔP^* values calculated point by point depend somewhat on blend composition as shown in *Figure 15b*. This may stem from the possibility that the cloud point, defined as the first sign of cloudiness, may not represent the spinodal at off-critical compositions. Because the spinodal and binodal curves converge at the critical point, such errors will be minimized there. The calculated critical point at ~70 wt% PPO corresponds to the minimum in *Figure 15a*. The interaction energy obtained at the critical point is $-0.10\,cal\,cm^{-3}$.

PPO was found to be immiscible with all α-MSAN copolymers in the available range of AN contents from 4 to 57.6 wt% AN. Blends were solution cast from tetrahydrofuran, chloroform and trichloroethylene. These

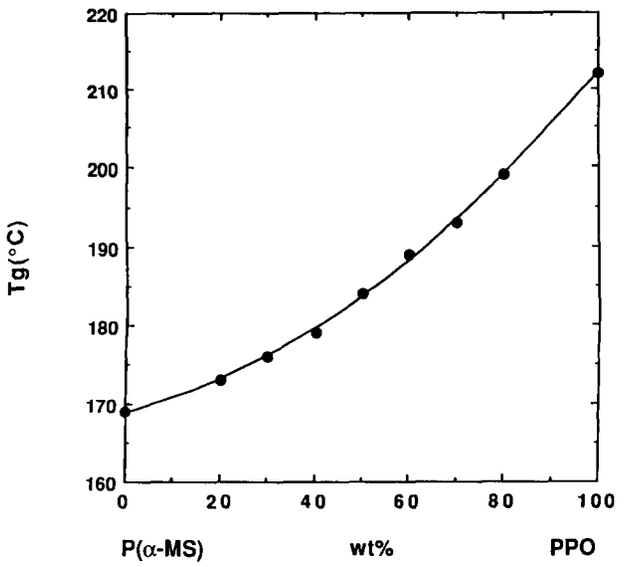

Figure 14 T_g behaviour for blends of P(α-MS) and PPO

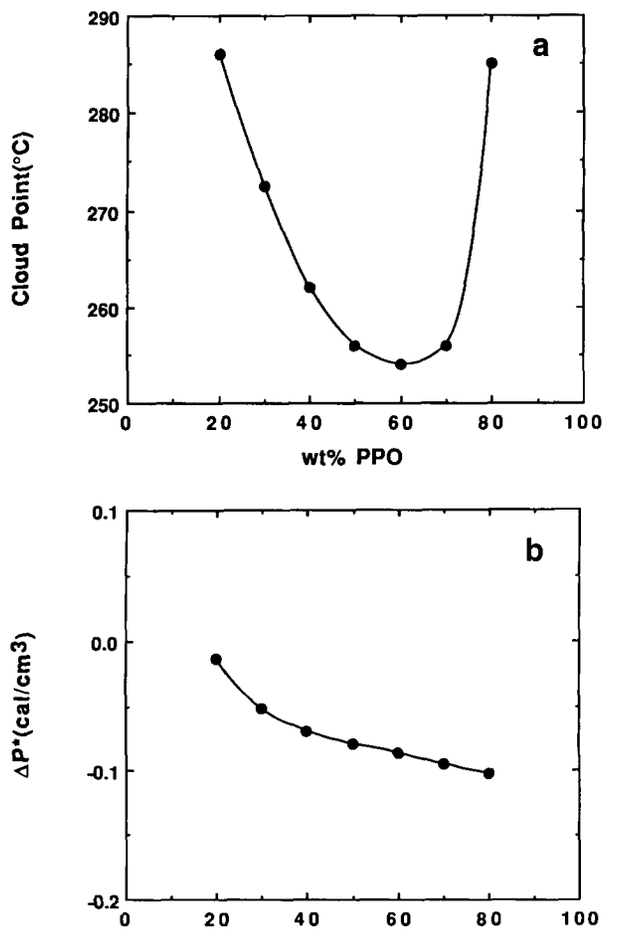

Figure 15 (a) Phase separation temperatures for blends of PPO with P(α-MS) and (b) ΔP^* calculated from the phase separation temperatures using the lattice-fluid theory

blends were also precipitated from the solvents described earlier into methanol. Thus, this observation is probably not an artifact of the preparation procedure. Copolymerization with AN evidently is not a useful way to raise the low phase separation temperatures of PPO/P(α-MS) blends.

Using $\Delta P^*_{\alpha\text{-MS/AN}} = 8.60$ and $\Delta P^*_{\alpha\text{-MS/PPO}} = -0.10\,\text{cal cm}^{-3}$, $\Delta P^*_{\text{PPO/AN}}$ can be estimated to be greater than $10.15\,\text{cal cm}^{-3}$ on the basis that the *LCST* spinodal for a PPO blend with α-MSAN4 must lie below the drying temperature of 200°C used here. The corresponding Flory–Huggins B_{ij} values calculated at 25°C are $B_{\alpha\text{-MS/PPO}} = -0.06$ and $B_{\text{PPO/AN}} = 9.91\,\text{cal cm}^{-3}$. On the other hand, blends of PPO have been reported by Kressler *et al.*[17] to be miscible with SAN copolymers containing less than 12.4 wt% AN. For AN contents in the range of 9.8 to 12.4 wt%, *LCST* behaviour occurs, but at lower AN contents the blends did not phase separate prior to decomposition. From the work of Kressler *et al.*[17], blends of PPO and SAN11 are estimated to phase separate at about 200°C, from which we can calculate $\Delta P^* \simeq -0.03\,\text{cal cm}^{-3}$. This leads to the following estimate: $\Delta P^*_{\text{S/PPO}} < -0.42\,\text{cal cm}^{-3}$ assuming that $\Delta P^*_{\text{S/AN}} = 7.37$ and $\Delta P^*_{\text{PPO/AN}} > 10.2\,\text{cal cm}^{-3}$. The Flory–Huggins B_{ij} computed at 25°C for S/PPO is less than $-0.41\,\text{cal cm}^{-3}$, which is consistent with the previous reports[26,66].

Using α-methylstyrene instead of styrene in AN copolymers severely limits the amount of AN that can be incorporated while maintaining miscibility with PPO. While $\Delta P^*_{\alpha\text{-MS/AN}} > \Delta P^*_{\text{S/AN}}$, $\Delta P^*_{\text{S/PPO}}$ is more negative than $\Delta P^*_{\alpha\text{-MS/PPO}}$, based on the observations that blends of PPO with PS evidently have a higher phase separation temperature than do blends with P(α-MS). Since $\Delta T^*_{\alpha\text{-MS/PPO}} = 69$°C and $\Delta T^*_{\text{S/PPO}} = 52$°C are relatively similar, the dominant factor that alters the phase behaviour for blends with PPO is evidently ΔP^*_{ij} rather than ΔT^*_{ij}.

Blends with PCL

Poly(ε-caprolactone) (PCL) forms miscible blends with SAN copolymers containing 8 to 28 wt% AN[69–72]. Phase separation temperatures from the work of Chiu *et al.*[71] (full circles in *Figure 16a*) were used here to calculate interaction energies for this system. As before, the open circles represent immiscible blends. The ΔP^* values shown in *Figure 16b* were calculated using the characteristic equation-of-state parameters for PCL[13] shown in *Table 2*. Assuming $\Delta P^*_{\text{S/AN}} = 7.37\,\text{cal cm}^{-3}$ (ref. 14), fitting of equation (9) to these values gives $\Delta P^*_{\text{S/PCL}} = 0.07$ and $\Delta P^*_{\text{PCL/AN}} = 4.43\,\text{cal cm}^{-3}$. The full curve in *Figure 16a* is the locus of spinodal temperatures calculated from the ΔP^* full curve in *Figure 16b*. The spinodal curve coincides with the experimental phase behaviour rather well. The Flory–Huggins B_{ij} at 60°C from the above ΔP^*_{ij} are $B_{\text{S/PCL}} = 0.09$, $B_{\text{PCL/AN}} = 4.62$ and $B_{\text{S/AN}} = 7.16\,\text{cal cm}^{-3}$, respectively. The corresponding curve for B calculated using these B_{ij} values is shown in *Figure 16b*.

None of the α-MSAN copolymers listed in *Table 1* or P(α-MS) proved to be miscible with PCL. Blends were solution cast or precipitated from THF, chloroform or trichloroethylene into methanol. Two T_g values were obtained by d.s.c. and the films were cloudy even after heating above the PCL melting temperature. Since equation-of-state effects are only modestly greater for α-MSAN copolymers ($\Delta T^*_{\alpha\text{-MS/PCL}} = 91$°C *versus* $\Delta T^*_{\text{S/PCL}} = 74$°C), the lack of miscibility of PCL with α-MSAN copolymers must reflect more unfavourable values of ΔP^* than exist for PCL/SAN. This combined with the fact that $\Delta P^*_{\alpha\text{-MS/AN}} = 8.60$ *versus* $\Delta P^*_{\text{S/AN}} = 7.37\,\text{cal cm}^{-3}$ leads to the conclusion that $\Delta P^*_{\alpha\text{-MS/PCL}} > \Delta P_{\text{S/PCL}} = 0.07\,\text{cal cm}^{-3}$.

Blends with PC

It is well known that bisphenol-A polycarbonate (PC)

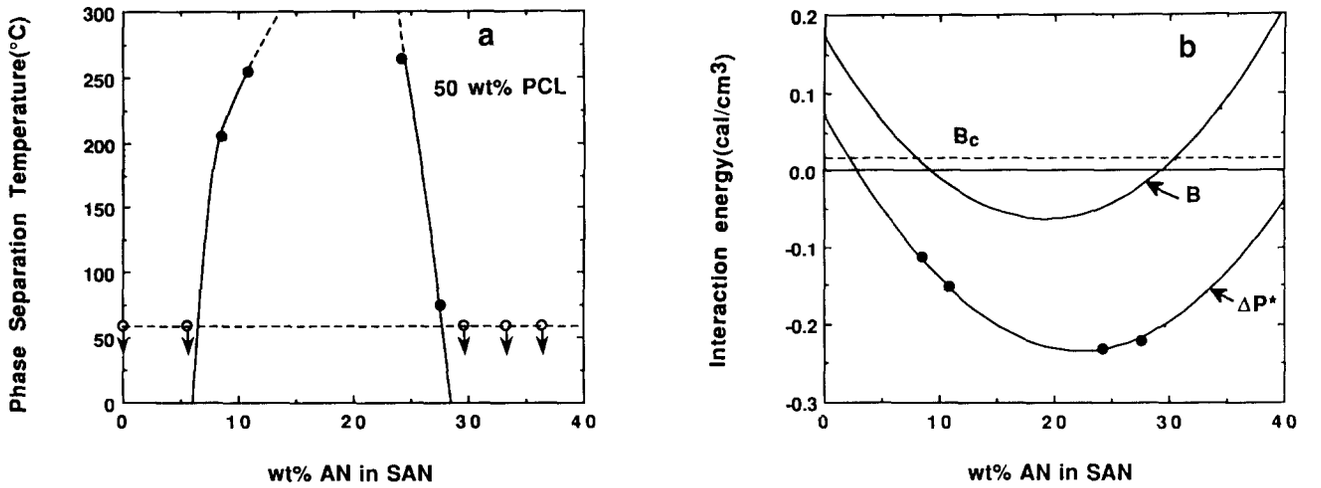

Figure 16 (a) Phase separation temperatures and (b) bare interaction parameters for 50/50 PCL/SAN blends using data from Chiu *et al.*[71]. The broken line in (a) represents the blend melting temperature. The full curve in (a) shows the estimated spinodal temperatures using equation (9) for ΔP^*, while the full circles are the experimentally determined phase separation temperatures. Arrows on the open circles correspond to blends with phase separation temperatures below the melting temperature. The full curves in (b) show the interaction energies calculated from the predicted B_{ij} and ΔP^*_{ij} values, while points are the ΔP^* determined from the experimental phase diagram using the lattice-fluid theory

Table 3 Comparison of estimated cohesive energy parameters and interaction energies

(a) Homopolymer cohesive energy parameters $((\text{cal cm}^{-3})^{1/2})$

Polymer	Abbreviations	δ	$(P^*)^{1/2}$
Poly(methyl methacrylate)	PMMA	9.1	11.0
Polystyrene	PS	9.5	9.8
Poly(α-methylstyrene)	PαMS	9.1	10.1
Tetramethylbisphenol A polycarbonate	TMPC	9.5	10.3
Polyacrylonitrile	PAN	13.8	11.4
Poly(vinyl chloride)	PVC	9.9	10.0
Poly(2,6-dimethyl-1,4-phenylene oxide)	PPO	9.8	9.9
Poly(ε-caprolactone)	PCL	9.4	10.1

(b) Interaction energies $((\text{cal cm}^{-3})^{1/2})$

Interaction pair	ΔP^*_{ij}	$[(P^*_i)^{1/2})-(P^*_j)^{1/2}]^2$	B_{ij}[a]	$(\delta_i-\delta_j)^2$ by Coleman[5]
S/AN	7.37	2.50	7.02(120)	18.5
α-MS/AN	8.60	1.69	7.96(150)	22.4
S/MMA	0.23	1.51	0.23(120)	0.16
α-MS/MMA	0.02	0.90	0.12(150)	0.00
S/TMPC	−0.17	0.26	−0.14(160)	0.00
α-MS/TMPC	0.01	0.05	0.18(180)	0.21
S/VC	0.17 to 0.40	0.02	0.16 to 0.38(100)	0.16
α-MS/VC	0.26	0.08	0.37(130)	0.70
S/PPO	< −0.42	0.01	< −0.41(25)	0.08
α-MS/PPO	−0.10	0.04	−0.06(25)	0.52
S/PCL	0.07	0.08	0.09(60)	0.01
α-MS/PCL	> 0.07	0.00	> 0.09(60)	0.10
MMA/AN	4.44	0.12	4.32(150)	22.1
TMPC/AN	5.92	1.14	5.67(180)	18.5
VC/AN	4.30	2.05	4.24(130)	15.2
PPO/AN	> 10.2	2.28	> 9.91(25)	16.1
PCL/AN	4.43	1.66	4.62(60)	19.5

[a] Note that B_{ij} represent values from the spinodal condition evaluated at the temperatures (°C) shown in parentheses

Table 4 Interaction parameters (cal cm^{-3}) for various monomer pairs

Interaction pair	This paper					Other sources		
	ΔP_{ij}^*	B_{ij} (at T°C)	ΔP_{ij}^*	B_{ij}	χ_{ij}	System[a]	Method[b]	References
S/AN	–	7.02 (120)	7.37	–	–	TMPC/SAN	A	14
				6.74	–	PMMA/SAN	B	1
			–	8.14	–	PMMA/SAN	B	2
			–	8.02	–	SAN/MMA copolymers with PhMA, CHMA or tBMA	B	48
			–	6.8	–	SAN/CHMA/MMA copolymers	B	18
			–	4.99	–	PMMA/SAN	B	6
			–	8.0	–	SAN/SAN	B	74
αMS/AN	8.60	7.96 (150)	–	5.33 (intra)	–	PMMA/α-MSAN	B	8
			–	6.03 (inter)	–	α-MSAN/SAN	B	9
S/MMA	0.23	0.23 (120)	0.30–0.36	–	–	PMMA/PS	C	54
			0.25	0.19	–	TMPC/SMMA	A	14
			–	0.13	–	MMA/CHMA copolymers/PS	B	2
			–	0.18	–	PMMA/PS/solvent	D	33–35
αMS/MMA	0.02	0.12 (150)	–	0.11	–	PMMA/α-MSAN	B	8
MMA/AN	4.36	4.32 (150)	–	3.18	–	PMMA/α-MSAN	B	8
			–	4.11	–	PMMA/SAN	B	1
			–	4.78	–	SAN/MMA copolymers with PhMA, CHMA or tBMA	B	48
S/TMPC	−0.17	−0.14 (160)	−0.17	–	–	TMPC/PS	A	15
αMS/TMPC	0.005	0.18 (180)	–	–	–			
TMPC/AN	5.92	5.67 (180)	5.92	6.01 (30)	–	TMPC/SAN	A	14
S/VC	0.17–0.40	0.16–0.38 (100)	–	–	–			
αMS/VC	0.26	0.37 (130)	–	–	–			
VC/AN	4.30	4.24 (130)	–	–	–			
S/PPO	< −0.42	< −0.41 (25)	–	–	−0.1	PPO/PS	B	10
				−0.8		PPO/PS	B	65
αMS/PPO	−0.10	0.06 (25)	–	–	–			
PPO/AN	> 10.5	> 9.91 (25)	–	–	0.5	PPO/SAN	B	17
S/PCL	0.07	0.09 (60)	–	–	–			
αMS/PCL	> 0.07	> 0.09 (60)	–	–	–			
PCL/AN	4.44	4.62 (60)	–	–	–			

[a] Abbreviations: PhMA, phenyl methacrylate; CHMA, cyclohexyl methacrylate; tBMA, t-butyl methacrylate
[b] A = Analysis of *LCST*-type phase diagram. B = Analysis of copolymer miscibility boundaries. C = Analysis of critical molecular-weight observations, D = Analysis of light scattering from polymer/polymer/solvent mixtures

is not miscible with polystyrene or with SAN copolymers[73,74]. None of the α-MSAN copolymers used in this work were found to be miscible with PC including a low-molecular-weight PC sample with $\bar{M}_w = 9900$.

Interaction parameters obtained via solubility-parameter theory

Table 3 lists for each homopolymer the solubility parameters estimated using the group contribution method described by Coleman *et al.*[5] and the square root of the characteristic pressure obtained by fitting the Sanchez–Lacombe equation of state[44–46] to experimental *PVT* data above T_g. The following equations provide estimates for the interaction energies B_{ij} and ΔP_{ij}^*:

$$B_{ij} = (\delta_i - \delta_j)^2 \tag{14}$$

or

$$\Delta P_{ij}^* = [(P_i^*)^{1/2} - (P_j^*)^{1/2}]^2 \tag{15}$$

for the simple case when the i–j interaction is equal to the geometric mean of those for the two like pairs i–i and j–j (i.e. the case of non-polar dispersive interactions). In general, equations (14) and (15) do not provide very good estimates for the B_{ij} and ΔP_{ij}^* values deduced from phase behaviour.

SUMMARY

This study demonstrates that the phase behaviour of blends of styrene/acrylonitrile copolymers with a number of homopolymers is different when the styrene monomer is replaced with α-methylstyrene monomer. The changes observed are specific to each system. The use of α-methylstyrene instead of styrene in copolymers with acrylonitrile broadens the miscibility window for blends with PMMA and PVC, but narrows the window for blends with TMPC. Phase separation temperatures are increased for blends with PVC but decreased for blends with PMMA and TMPC. PPO, PCL and low-molecular-weight PC were found to be immiscible with α-MSAN copolymers at all available AN compositions.

The interaction energy densities that govern the phase behaviour of copolymer–homopolymer systems were determined from phase separation temperature data using the Sanchez–Lacombe lattice-fluid theory and a binary interaction model. This method of analysis, in principle, allows independent determination of the interaction energy densities for all three pairs of repeat units, whereas analysing the copolymer composition limits of the miscible range using the Flory–Huggins theory and the binary interaction model can only give two interaction energies assuming a third is known from other sources. However, in some cases of limited data, the present method cannot be used to extract reliably all the pertinent pairs of interaction energies as found for some systems examined here.

Table 4 lists all Sanchez–Lacombe ΔP^*_{ij} and Flory–Huggins B_{ij} values obtained from this study and compares them to those obtained from other sources. In some cases ΔP^*_{ij} were obtained independently from two separate systems (e.g. $\Delta P^*_{MMA/AN}$ and $\Delta P^*_{\alpha\text{-MS/AN}}$), and the two values agreed well. The $\Delta P^*_{S/MMA}$ calculated here for blends of PMMA/SAN is similar to the value obtained from analysis of TMPC/SMMA blends[14]. Such agreement serves to demonstrate the validity of the interaction energies calculated. In addition, the B_{ij} values computed from ΔP^*_{ij} show relatively good agreement with values deduced from analysis of miscibility boundaries (e.g. $B_{MMA/AN}$). The changes in phase diagram of blends observed when α-methylstyrene is substituted for styrene in AN copolymers can be attributed to either interaction energies (ΔP^*) or equation-of-state effects (ΔT^*) or to both. No generalization could be made for the change in magnitude of ΔP^*_{ij} values when styrene is replaced by α-methylstyrene. However, ΔT^*_{ij} are generally larger when α-methylstyrene is substituted for styrene in AN copolymers because the T^* value for P(α-MS) is higher than that compared to polystyrene. In general, this study extends the database of interaction energy densities, which will allow prediction of phase behaviour for other polymer blend systems.

ACKNOWLEDGEMENTS

Financial support of this work has been provided by the Air Force Office of Scientific Research and by the National Science Foundation Grant Numbers DMR-89-00704 and DMR-92-15926 administered by the Division of Material Research—Polymers Program. A. R. Padwa wishes to thank Monsanto Company for permission to publish these results.

REFERENCES

1 Nishimoto, M., Keskkula, H. and Paul, D. R. *Polymer* 1989, **30**, 1279
2 Brannock, G. R., Barlow, J. W. and Paul, D. R. *J. Polym. Sci., Polym. Phys. Edn* 1990, **28**, 871
3 Brannock, G. R. PhD Dissertation, University of Texas at Austin, 1990
4 Brannock, G. R., Barlow, J. W. and Paul, D. R. *Macromolecules* 1991, **29**, 413
5 Coleman, M. M., Graf, J. F. and Painter, P. C. 'Specific Interactions and the Miscibility of Polymer Blends', Technomic, Lancaster, PA, 1991
6 Cowie, J. M. G. and Lath, D. *Makromol. Chem., Macromol. Symp.* 1988, **16**, 104
7 Cowie, J. M. G. *J. Polym. Sci., Polym. Phys. Edn* 1991, **29**, 207
8 Cowie, J. M. G. and Elexpuru, E. M. *Eur. Polym. J.* 1992, **28**, 623
9 Cowie, J. M. G., Elexpuru, E. M. and McEwen, I. J. *Polymer* 1992, **33**, 1993
10 Kambour, R. P., Bendler, J. T. and Bopp, R. C. *Macromolecules* 1983, **16**, 753
11 Walsh, D. J., Higgins, J. S. and Maconnachie, A. (Eds) 'Polymer Blends and Mixtures', Reidel, Dordrecht, 1985
12 Karasz, F. E. and MacKnight, W. J. *Adv. Chem. Ser.* 1986, **211**, 67
13 Kim, C. K. PhD Dissertation, University of Texas at Austin, 1992
14 Kim, C. K. and Paul, D. R. *Polymer* 1992, **33**, 2089
15 Kim, C. K. and Paul, D. R. *Polymer* 1992, **33**, 1630
16 Kressler, J., Kammer, H. W. and Klostermann, K. *Polym. Bull.* 1986, **15**, 113
17 Kressler, J. and Kammer, H. W. *Acta Polym.* 1987, **11**, 600
18 Nishimoto, M., Keskkula, H. and Paul, D. R. *Macromolecules* 1990, **23**, 3633
19 Kang, H. S., MacKnight, W. J. and Karasz, F. E. *Polym. Prepr. (Am. Chem. Soc. Div. Polym. Chem.)* 1987, **28**, 134
20 Goh, S. H., Paul, D. R. and Barlow, J. W. *Polym. Eng. Sci.* 1982, **22**, 34
21 Goh, S. H. and Siow, K. S. *J. Appl. Polym. Sci.* 1984, **29**, 99
22 Goh, S. H. and Siow, K. S. *J. Appl. Polym. Sci.* 1986, **32**, 3407
23 Goh, S. H., Lee, S. Y. and Siow, K. S. *J. Appl. Polym. Sci.* 1986, **31**, 2055
24 Goh, S. H., Lee, S. Y., Siow, K. S. and Pua, C. L. *J. Appl. Polym. Sci.* 1987, **33**, 353
25 Goh, S. H. *Polym. J.* 1990, **26**, 1149
26 Weeks, N. E., Karasz, F. E. and MacKnight, W. J. *J. Appl. Phys.* 1977, **48**, 4068
27 Fowler, M. E., Barlow, J. W. and Paul, D. R. *Polymer* 1986, **28**, 1177
28 Kim, J. H., Barlow, J. W. and Paul, D. R. *J. Polym. Sci., Polym. Phys. Edn* 1989, **27**, 223
29 Kim, J. H., Barlow, J. W. and Paul, D. R. *Polym. Eng. Sci.* 1989, **29**, 581
30 Kim, J. H., Barlow, J. W. and Paul, D. R. *J. Polym. Sci., Polym. Phys. Edn* 1989, **27**, 2211
31 Shiomi, T., Karasz, F. E. and MacKnight, W. J. *Macromolecules* 1986, **19**, 2274
32 Kim, J. H. PhD Dissertation, University of Texas at Austin, 1989
33 Fukuda, T. and Inagaki, H. *Pure Appl. Chem.* 1983, **55**, 1541
34 Fukuda, T., Nagata, M. and Inagaki, H. *Macromolecules* 1984, **17**, 548
35 Fukuda, T., Nagata, M. and Inagaki, H. *Macromolecules* 1986, **19**, 1411
36 Brannock, G. R. and Paul, D. R. *Macromolecules* 1990, **23**, 5240
37 McCormick, H. W. *J. Polym. Sci.* 1957, **25**, 488
38 Suess, M., Kressler, J., Kammer, H. W. and Heinemann, K. *Polym. Bull.* 1986, **16**, 371
39 Flory, P. J. 'Principles of Polymer Chemistry', Cornell University Press, Ithaca, NY, 1953
40 Sanchez, I. C. *Polymer* 1989, **30**, 471
41 Paul, D. R. and Barlow, J. W. *Polymer* 1984, **25**, 487
42 ten Brinke, G. and Karasz, F. E. *Macromolecules* 1984, **17**, 815
43 Lacombe, R. H. and Sanchez, I. C. *J. Phys. Chem.* 1976, **80**, 2268
44 Sanchez, I. C. and Lacombe, R. H. *J. Phys. Chem.* 1976, **80**, 2352
45 Sanchez, I. C. and Lacombe, R. H. *J. Polym. Sci., Polym. Lett. Edn* 1977, **15**, 71
46 Sanchez, I. C. and Lacombe, R. H. *Macromolecules* 1978, **11**, 1145
47 Callaghan, T. A. PhD Dissertation, University of Texas at Austin, 1992

48 Gan, P. P. PhD Dissertation, University of Texas at Austin, 1993
49 Paul, D. R. and Newman, S. E. 'Polymer Blends', Academic Press, New York, 1987
50 Stein, D. J., Jung, R. H., Illers, K. H. and Hendus, H. *Angew. Makromol. Chem.* 1974, **36**, 89
51 Chiou, J. S., Paul, D. R. and Barlow, J. W. *Polymer* 1982, **23**, 1543
52 Naito, K., Johnson, G. E., Allara, K. L. and Kwei, T. K. *Macromolecules* 1978, **11**, 1260
53 Bernstein, R. E., Cruz, C. A. and Paul, D. R. *Macromolecules* 1977, **10**, 681
54 McMaster, L. P. *Adv. Chem. Ser.* 1975, **142**, 43
55 Callaghan, T. A. and Paul, D. R. *Macromolecules* 1993, **26**, 2439
56 Bank, M., Leffingwell, J. and Thies, C. *Macromolecules* 1971, **43**, 1971
57 Patterson, D. *Polym. Eng. Sci.* 1984, **22**, 64
58 Robard, A. and Patterson, D. *Macromolecules* 1977, **10**, 1021
59 Robard, A. and Patterson, D. *Macromolecules* 1977, **10**, 706
60 Nishimoto, M. Keskkula, H. and Paul, D. R. *Polymer* 1991, **32**, 272
61 Rodgers, P. A. *J. Appl. Polym. Sci.* 1993, **48**, 1061
62 Albert, B., Jerome, R. and Teyssie, P. *J. Polym. Sci., Polym. Chem. Edn* 1986, **24**, 551
63 Buchdahl, R. and Nielsen, L. E. *J. Polym. Sci.* 1955, **15**, 1
64 Schneider, I. A. and Calugaru, E. M. *Eur. Polym. J.* 1976, **12**, 879
65 Schultz, A. R. and Gendron, B. M. *J. Appl. Polym. Sci.* 1972, **16**, 461
66 Tucker, P. S. and Paul, D. R. *Macromolecules* 1988, **21**, 2801
67 Stoelting, J., Karasz, F. E. and MacKnight, W. J. *Polym. Eng. Sci.* 1970, **10**, 133
68 Kambour, R. P., Bendler, J. T. and Bopp, R. C. *Macromolecules* 1983, **16**, 753
69 Runt, J. and Rim, P. B. *Macromolecules* 1982, **15**, 1018
70 Rim, P. B. and Runt, J. P. *Macromolecules* 1983, **16**, 762
71 Chiu, S. C. and Smith, T. G. *J. Appl. Polym. Sci.* 1984, **29**, 1797
72 Chiu, S. C. and Smith, T. G. *J. Appl. Polym. Sci.* 1984, **29**, 1781
73 Mendelson, R. A. *J. Polym. Sci., Polym. Phys. Edn* 1985, **23**, 1975
74 Keitz, J. D., Barlow, J. W. and Paul, D. R. *J. Appl. Polym. Sci.* 1984, **29**, 3131